A Fast Solver for Stokes Flow in 2D: [this is a bad title]

Haiyang Wang, Nils Jan Fredrik Fryklund, Samuel Potter, Leslie Greengard

November 17, 2022

Abstract

In this paper, we exploit the *return to Poiseuille* phenomenon: a Stokes flow would quickly developed into the Poiseuille flow along a straight channel. This allows us to quickly solve the interior plane Stokes equation on a domain that is union of *standard pieces*. Each standard piece's is a pipe with inlets/outlets being long enough straight channels, such that when two standard pieces are connecting, the velocity profile at where they connect would be close to Poiseuille flow velocity profile within machine precision. [1] Therefore, instead of solving stokes equation for the global domain, we can solve the Stokes equation for each standard pieces with Poiseuille boundary condition at inlets/outlets, and easily interface these local solutions to build a solution for the global domain.

Once the Stokes equation with Poiseuille boundary conditions is pre-solved on each standard piece, the standard pieces can be connected to form a complex channel network. Interfacing the solutions of standard pieces would instantly give us a high-order accurate solution of Stokes equation for the global domain of the channel network. The interfacing is based on the physics constraints of zero-net-flux and continuity of pressure. These constraints can be written as a full rank linear system of rank $O(n)$, where n is the number of standard pieces. Thus, connecting the local solvers would have time complexity of $O(n^2)$. This is much faster than solving the global problem directly. For example, in Figure 1, interfacing the local solutions took only 0.3 seconds, while directly solving on the global domain took 24 minutes.

1 Introduction

The *return to Poiseuille* phenomenon, or *Saint-Venant's principle* in the theory of plane elasticity, are well-established from the last century [3, 6, 8]. To be more specific, in a straight channel with laminar and incompressible incoming flow, the differences of Stokes flow and Poiseuille flow would decay exponentially fast toward the outlet. Therefore it is a good numerical hypothesis to assume that the flow is Poiseuille in middle of a lone straight channel.

For plane Stokes flow, the biharmonic equation formulation are well known and developed within theory of complex variable from the last century [9]. Various numerical schemes, such as boundary integral equation (BIE) and rational function approximation, have been developed accordingly [5, 13].

In this paper, we use the biharmonic BIE formulation for the plane Stokes equation from [5] to solve the Stokes equation on several standard pieces with Poiseuille boundary condition at inlets/outlets. The biharmonic BIE is coupled with a Fast Multiple Method (FMM) for 2D biharmonic equation to reduce the time and space complexity of solving the BIE. [1]

Directly evaluating the BIE's solution near the boundary could be numerically unstable as the integral is nearly-singular. Thus, we have adopted the methods from [14, 7] to for accurate evaluation of layer potentials near the boundary.

Interfacing the local solutions of each standard pieces is by simply solving a system of linear equations, based on the constraints of zero-net-flux and continuity of pressure. This linear equation depends merely on the flux and pressure at the point of connection of standard pieces.

This paper is organized as follows. In Section 2, we define the Stokes boundary value problem, the corresponding biharmonic boundary value problem, and then the integral equation of it. We also mention the analytic evidence for the *return to Poiseuille* hypothesis. In Section 3, we presents the Nyström discretization of the integral equation. The numerical experiments of connecting standard pieces and numerical evidence for *return to Poiseuille* hypothesis are contained in Section 4, followed by conclusions in Section 5.

2 Mathematical Preliminaries

In this section, we briefly review the Stokes equation, its biharmonic form, and the biharmonic boundary integral equation. More detailed discussion can be found in [5]. Then, we will present an analytic estimate for the exponential decay rate of *return to Poiseuille* [6], and explain how have used it as a numerical hypothesis in this paper.

2.1 Boundary Integral Equation

Stokes Boundary Value Problem The plane linear Stokes equations are

$$\nu \Delta u = \frac{1}{\rho}\frac{\partial p}{\partial x}, \quad \nu \Delta v = \frac{1}{\rho}\frac{\partial p}{\partial y} \tag{1}$$

$$\frac{\partial u}{\partial x} + \frac{\partial v}{\partial y} = 0 \tag{2}$$

where u, v are components of velocity, ρ is the density, ν is the viscosity, and p is the pressure. Another important physics quantity, vorticity, is defined as $\zeta = u_y - v_x$.

We are interested in Dirichlet boundary value problem of Stokes equation on a bounded $(M+1)$-ply connected domain $D \subset \mathbb{R}^2$, with boundary $\partial D = \Gamma = \Gamma_0 \cup \Gamma_1 \cup \cdots \cup \Gamma_M$, where Γ_0 is the exterior boundary, and $\Gamma_1, \cdots, \Gamma_M$ are the interior boundaries. On the boundary Γ, the velocity is defined by

[1] The length of straight channel is greater than 7 times of the width, as indicated by Figure 2

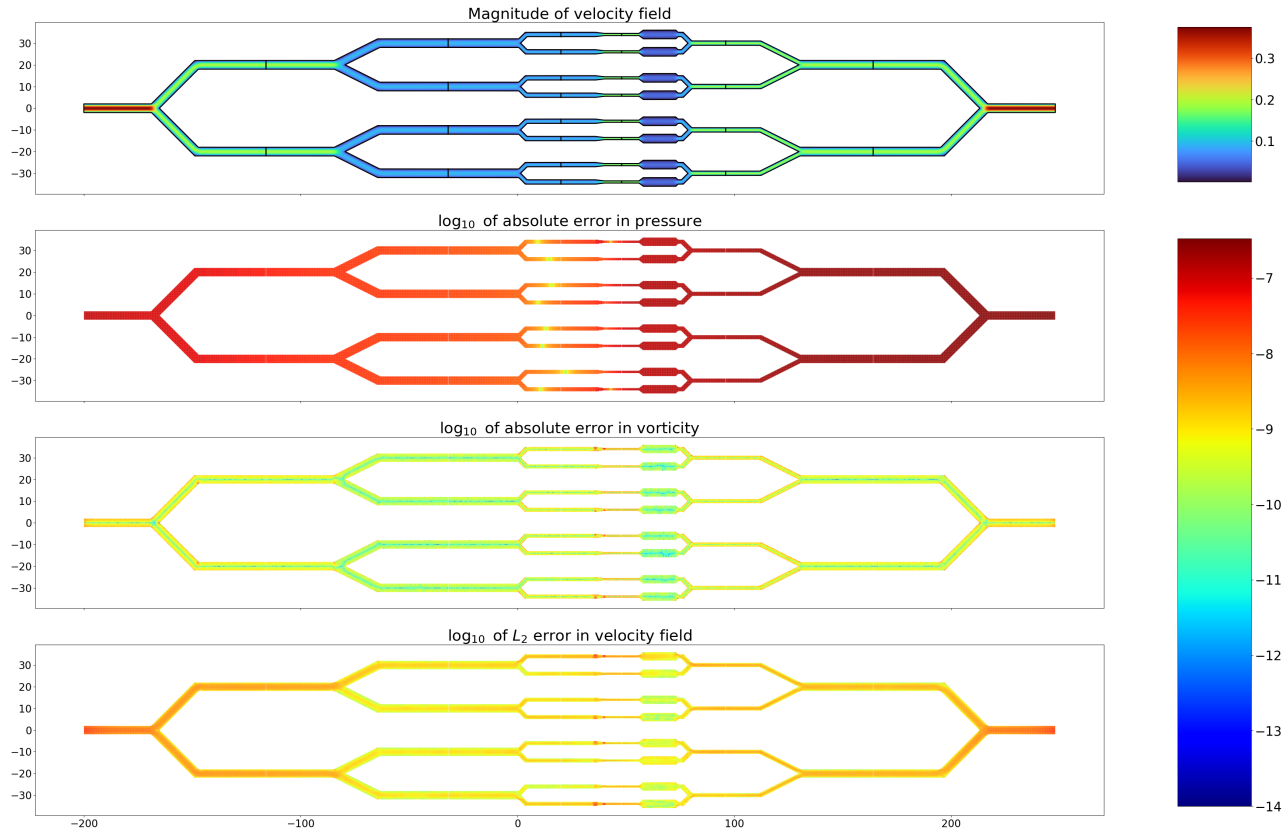

Figure 1: Solutions of the Stokes equation in a complex channel geometry as a union of 22 standard pieces with Dirichlet Boundary conditions, and the difference between connected local solution with the global solution. The first sub-figure is a color-plot of magnitude of velocity field inside the domain, with colorbar on its right. The black lines in the first sub-figure marks the boundary of each standard pieces. The other three sub-figures is color plot of absolute differences between the connected solutions and a global solution in terms of pressure, vorticity, and velocity field in the log_{10} scale. Each standard pieces are solved with required accuracy of 10^{-12} and the global domain is solved with required accuracy of 10^{-10}.

given functions h_1, h_2:

$$u = h_2(t), \quad v = -h_1(t), \quad t \in \Gamma \tag{3}$$

Biharmonic Equation. (2) implies the existence of the stream function $W(x, y)$ such that:

$$\frac{\partial W}{\partial x} = -v, \quad \frac{\partial W}{\partial y} = u \tag{4}$$

Following (1,2), it is easy to see that the stream function satisfies the biharmonic equation (5), and the Dirichlet boundary condition of velocity (3) can be understood as the boundary conditions for the biharmonic equation (6):

$$\Delta^2 W(x, y) = \Delta\zeta = 0, \qquad (x, y) \in D \tag{5}$$

$$\frac{\partial W}{\partial x} = h_1(t), \quad \frac{\partial W}{\partial y} = h_2(t), \qquad t \in \Gamma \tag{6}$$

Goursat's Formula. It has been long established that any plane biharmonic function $W(x, y)$ can be expressed by Goursat's formula

$$W(x, y) = \mathrm{Re}(\bar{z}\phi(z) + \chi(z)) \tag{7}$$

where ϕ, χ are referred to as the Goursat's functions, and are analytic functions of complex variable $z = x + yi$. In the following, we will be identifying $(x, y) \in \mathbb{R}^2$ with $x + yi$.

Velocity, pressure, and vorticity can be conveniently expressed with the Goursat's functions. The Muskhelishvili's formula (8) expresses velocity field and another formula (9) gives the pressure and vorticity:

$$-v + ui = \frac{\partial W}{\partial x} + i\frac{\partial W}{\partial y} = \phi(z) + z\overline{\phi'(z)} + \overline{\psi(z)} \tag{8}$$

$$\zeta + \frac{i}{\nu}p = 4\phi'(z) \tag{9}$$

where $\psi = \chi'$ [11].

The biharmonic boundary value problem (5,6), using the Muskhelishvili's formula (8), can be rewritten as

$$\phi(t) + t\overline{\phi'(t)} + \overline{\psi(t)} = h(t), \quad t \in \Gamma \tag{10}$$

where $h(t) = h_1(t) + ih_2(t)$, and t is understood as a complex variable.

Sherman-Lauricella Representation. The boundary integral equation is an ansatz based on of an extension of Sherman-Lauricella representation for Stokes equation proposed in [5]. It is formulated as follows:

$$\phi(z) = \frac{1}{2\pi i}\int_\Gamma \frac{\omega(\xi)}{\xi - z}d\xi + \sum_{k=1}^{M} C_k \log(z - z_k) \tag{11}$$

$$\psi(z) = \frac{1}{2\pi i}\int_\Gamma \frac{\overline{\omega(\xi)}d\xi + \omega(\xi)\overline{d\xi}}{\xi - z} - \frac{1}{2\pi i}\int_\Gamma \frac{\overline{\xi}\omega(\xi)}{(\xi - z)^2}d\xi + \sum_{k=1}^{M}\left(\frac{b_k}{z - z_k} + \overline{C}_k \log(z - z_k) - C_k\frac{\overline{z}_k}{z - z_k}\right) \tag{12}$$

where ω is an unknown complex density on Γ to be solved for, z_k are arbitrarily prescribed point inside the component curves Γ_k, and C_k, b_k are constants defined by

$$C_k = \int_{\Gamma_k} \omega(\xi)|d\xi|, \quad b_k = 2\,\mathrm{Im}\int_{\Gamma_k}\overline{\omega(\xi)}d\xi \tag{13}$$

Boundary Integral Equation. Letting a point z in the interior of D approach to a point on the boundary $t \in \Gamma$, the classical formulae for the limiting values of Cauchy-type integral gives us the an integral equation for ω [10, 5] :

$$\begin{aligned}\omega(t) &+ \frac{1}{2\pi i}\int_\Gamma \omega(\xi) d\ln\frac{\xi - t}{\overline{\xi - t}} - \frac{1}{2\pi i}\int_\Gamma \overline{\omega(\xi)}d\frac{\xi - t}{\overline{\xi - t}} \\ &+ \sum_{k=1}^{M}\left(\frac{\overline{b}_k}{\overline{t - z_k}} + 2C_k\log|t - z_k| + \overline{C_k}\frac{t - z_k}{\overline{t - z_k}}\right) \\ &+ \frac{\overline{b}_0}{\overline{t} - \overline{z}^*} \\ &= h(t)\end{aligned} \tag{14}$$

the extra term $\frac{\overline{b}_0}{\overline{t} - \overline{z}^*}$ vanishes when the zero-net-flux condition $\mathrm{Re}\int_\Gamma \bar{h}(t)dt = 0$ is satisfied. The invertibility of this integral equation is similar to the standard proof of invertibility for elasticity problems [11], hence omitted.

2.2 Return to Poiseuille

In this section, we will first show the analytic estimate for the *return to Poiseuille* phenomenon, which is based on eigenfunction analysis on a domain of a semi-infinite strip from the theory of plane elasticity [6]. Then, we explain how to apply the *return to Poiseuille* hypothesis.

Analytic Estimate for Return to Poiseuille. On the domain of a semi-infinite pipe $D_L = \{(x, y) \mid x \geq 0, |y| \leq L\}$, with the boundaries

$$\begin{aligned}\Gamma_L &= \Gamma_L^1 \cup \Gamma_L^2 \cup \Gamma_L^3 \\ &= \{(0, y)||y| \leq L\} \cup \{(x, L)|x \geq 0\} \cup \{(x, -L) \mid x \geq 0\}\end{aligned} \tag{15}$$

where Γ_L^2, Γ_L^3 are walls with the non-slippery boundary conditions, and Γ_L^1 is the inlet with boundary condition of an incoming laminar incompressible flow. Return to Poiseuille means that regardless of the boundary conditions on Γ_L^1, the flow's profile at $x = l$ will converge Poiseuille flow as l approaches to infinity.

Without lost of generality, assuming there is zero net flux across Γ_L^1, return to Poiseuille is equivalent to return to zero flow. The equation for this BVP is the following:

$$\frac{\partial W(x, y)}{\partial y} = W(x, y) = 0, \qquad (x, y) \in \Gamma_L^2 \cup \Gamma_L^3 \tag{16}$$

$$\frac{\partial W(0, y)}{\partial x} = f(y), \ \frac{\partial W(0, y)}{\partial y} = g(y), \quad (0, y) \in \Gamma_L^1 \tag{17}$$

where f, g satisfy $f(\pm L) = g(\pm L) = \int_{-L}^{L} g(y)dy = 0$.

This biharmonic BVP is identical to the "self-equilibrated" traction BVP in the theory of elasticity studied in [6, 8, 3]. When f''', g''' exist and are of bounded variation, this problem has a unique solution spanned by the Papkovich-Fadle eigenfunctions [6]. The first eigenfunction is dominated by $e^{-xk/2L}$, where

$$k \simeq 4.2$$

is the smallest positive real parts of the roots of the transcendental equation $\sin^2\lambda - \lambda^2 = 0$. This gives the decay rate of return to Poiseuille hypothesis, which agrees with our numerical experiment in Figure 2.

Application of Return to Poiseuille. TODO Given the analytic bound, it is easy to see that in a straight channel with length greater than 8 times of the channel width, we can expect the flow to be Poiseuille up to 14th digits accuracy. Therefore, it is appropriate to require the inlets/outlets of the standard pieces to be such straight channels, and then assign the Poiseuille boundary conditions on them.

The straight channels outlets would have two corners of right angle, making the geometry non-smooth. Such piecewise smooth geometry can be handled as in [14] with panel refinement near the corners. Here, we choose a different approach to avoid handling corners by adding superficial caps to the outlets. [this paragraph needs more elaboration and some figures perhaps].

3 Description of Numerical Methods

In this section, we will first present Nyström discretization of boundary integral equation (14), and then we briefly explain the discretization of the boundary, near boundary evaluation of layer potential, and the system of linear equations for pipe connections.

3.1 Boundary Integral equation

The boundary curve Γ_k is given by the parametrization $\Gamma_k = \{t^k(a) : a \in [A_k, A_{k+1}]\}$, and discretized into N_k points $t_i^k = t^k(a_i^k)$. Associate to each point t_j^k are the unknown complex density ω_j^k, the derivative $d_j^k = t^{k\prime}(a_j^k)$, and the quadrature weight w_j^k. In total, we have $N = \sum_{k=0}^{M} N_k$ points. Nyström discretization of (14) is

$$\omega_j^k + \sum_{m=0}^{M}\sum_{n=1}^{N_k} K_1(t_j^k, t_n^m)\omega_j^k + \sum_{m=0}^{M}\sum_{n=1}^{N_k} K_2(t_j^k, t_n^m)\overline{\omega_j^k} = h_j^k \tag{18}$$

where $h_j^k = h(t_j^k)$ and the kernels K_1, K_2 are given by

$$K_1(t_j^k, t_n^m) = \frac{1}{\pi}\,\mathrm{Im}\left(\frac{d_n^m}{t_n^m - t_j^k}\right) w_n^m + K_1^s(t_j^k, t_n^m) \tag{19}$$

$$K_2(t_j^k, t_n^m) = \frac{1}{\pi}\frac{\mathrm{Im}((t_n^m - t_j^k)\overline{d_n^m})}{(\overline{t_n^m - t_j^k})^2} w_n^m + K_2^s(t_j^k, t_n^m) \tag{20}$$

with K_1^s, K_2^s being:

$$K_1^s(t_j^k, t_n^m) = \delta_m w_n^m \left(\frac{i\overline{d_n^m}}{\overline{t_j^k - z_m}} + 2\log|t_j^k - z_m|\right) \tag{21}$$

$$K_2^s(t_j^k, t_n^m) = \delta_m w_n^m \left(-\frac{id_n^m}{\overline{t_j^k - z_m}} + \frac{t_j^k - z_m}{\overline{t_j^k - z_m}}\right) \tag{22}$$

where $\delta_m = 1$ excepts for $\delta_0 = 0$. In the limiting case of $t_j^k = t_n^m$, the corresponding value can be seen as the limiting value:

$$K_1(t_j^k, t_j^k) = \frac{w_j^k \kappa_j^k |d_j^k|}{2\pi} + K_1^s(t_j^k, t_j^k) \tag{23}$$

$$K_2(t_j^k, t_j^k) = -\frac{w_j^k \kappa_j^k (d_j^k)^2}{2\pi |d_j^k|} + K_2^s(t_j^k, t_j^k) \tag{24}$$

where κ_j^k is the signed quadrature at the point t_j^k.

The left hand side (LHS) of (18) for any density ω is evaluated by a biharmonic fmm [1]. And this Nyström discretization is regarded as an matrix equation, by separating the real part and imaginary part, and then solved iteratively using generalized minimum residual method GMRES [12].

Evaluation of the layer potentials near boundary is done as in [14].

3.2 Geometry of the Boundary

The key to spectral convergence of GMRES is to have smooth boundary, or for piecewise smooth boundary, one can use special treatment as in [14] to ensure the spectral convergence is preserved. Here for this paper, we focused on smooth geometry. We adopted the ideas from [4, 2] to smooth the corners of the boundary by convolution, and added superficial caps at the inlets and outlets. [insert a figure here]. The geometry is adaptively discretized into Gauss-Legendre panels, as described in [14].

4 Numerical Results and Discussion

4.1 Numerical evidence of return to poiseuille

The numerical evidence for return to Poiseuille phenomenon is demonstrated on a straight pipe of width 1 and length 8 as in Figure 2. On the left boundary, a smooth velocity profile is imposed. This velocity profile is an arbitrarily picked smooth function that satisfies the requirement of equation (17). On the rest of the curve, non-slippery condition is imposed.

Figure 2a shows that the rate of returning to the zero flow is agreed with the predicted rate from Section 2.2 up to 14th digits of accuracy. Figure 2b is a color plot where the color indicates the $\log_{10}$ of absolute value of the velocity, pressure, and vorticity.

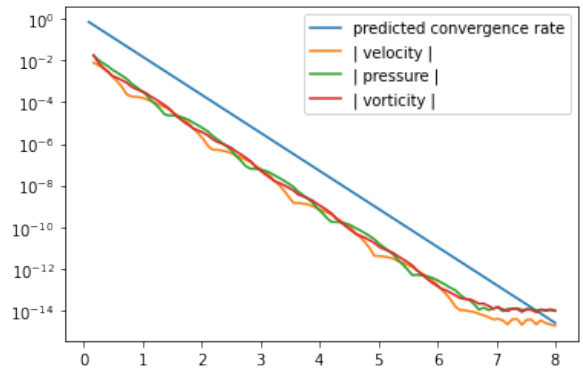

(a) Return to zero flow

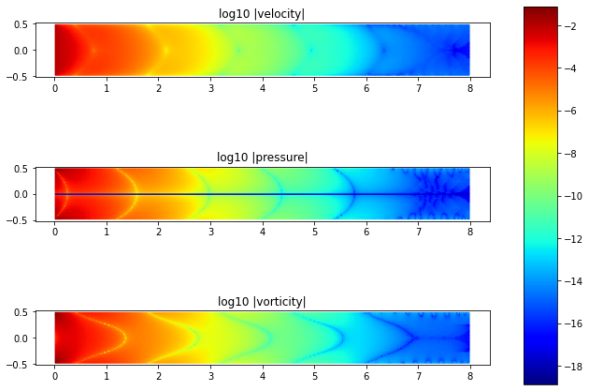

(b) Color plot of $\log_{10}$ of the absolute value of the velocity, vorticity, and pressure

Figure 2: Return to Poiseuille flow in a straight pipe.

4.2 a complicated network of pipes to show the power of this method

5 Conclusions

5.1 summarize what I've done

5.2 outlook. What other work might be followed?

References

[1] Flatironinstitute/fmm2d.

[2] Joar Bagge and Anna-Karin Tornberg. Highly accurate special quadrature methods for Stokesian particle suspensions in confined geometries. 93(7):2175–2224.

[3] Horgan Co. Recent developments concerning Saint-Venant's principle,". In *In Advances in Applied Mechanics, TY Wu and JW Hutchinson (Eds), Vol 23,*, pages 179–269. Academic Press,.

[4] Charles L. Epstein and Michael O'Neil. Smoothed corners and scattered waves.

[5] Leslie Greengard, Mary Catherine Kropinski, and Anita Mayo. Integral Equation Methods for Stokes Flow and Isotropic Elasticity in the Plane. 125(2):403–414.

[6] R. D. Gregory. The traction boundary value problem for the elastostatic semi-infinite strip; existence of solution,

and completeness of the Papkovich-Fadle eigenfunctions. 10(3):295–327.

[7] Johan Helsing and Rikard Ojala. On the evaluation of layer potentials close to their sources. 227(5):2899–2921.

[8] C. O. HORGAN. DECAY ESTIMATES FOR THE BIHARMONIC EQUATION WITH APPLICATIONS TO SAINT-VENANT PRINCIPLES IN PLANE ELASTICITY AND STOKES FLOWS. 47(1):147–157.

[9] O. A. Ladyzhenskaya, Richard A. Silverman, Jacob T. Schwartz, and Jacques E. Romain. *The Mathematical Theory of Viscous Incompressible Flow*. 17(2):57–58.

[10] Nikolaj I. Muschelišvili and Nikolaj I. Muschelišvili. *Singular Integral Equations: Boundary Problems of Function Theory and Their Application to Mathematical Physics*. Wolters-Noordhoff Publishing, softcover reprint of the original 1st ed. 1958 edition.

[11] N. I. Muskhelishvili. *Some Basic Problems of the Mathematical Theory of Elasticity*. Springer Netherlands.

[12] Youcef Saad and Martin H. Schultz. GMRES: A Generalized Minimal Residual Algorithm for Solving Nonsymmetric Linear Systems. 7(3):856–869.

[13] Lloyd N. Trefethen. *Approximation Theory and Approximation Practice, Extended Edition*. Society for Industrial and Applied Mathematics.

[14] Bowei Wu, Hai Zhu, Alex Barnett, and Shravan Veerapaneni. Solution of Stokes flow in complex nonsmooth 2D geometries via a linear-scaling high-order adaptive integral equation scheme. 410:109361.